Available online at www.sciencedirect.com
SCIENCE DIRECT®
Applied Thermal Engineering 24 (2004) 777–790
APPLIED THERMAL ENGINEERING
www.elsevier.com/locate/apthermeng

Performance investigation of plain circular and oval tube evaporatively cooled heat exchangers

Ala Hasan *, Kai Sirén

Laboratory of Heating, Ventilating and Air Conditioning, Helsinki University of Technology, P.O. Box 4400, FIN-02015 HUT, Finland

Received 23 April 2003; accepted 23 October 2003

Abstract

The performance of two evaporatively cooled heat exchangers is analysed, one has plain circular tubes while the other one has plain oval tubes. Both are investigated under similar operating conditions in relation to airflow rates and inlet hot water temperatures. The circular tube is 10 mm o.d., and the oval tube (axes ratio 3.085) is formed from an 18 mm o.d. circular tube whose perimeter is preserved after forming. It is concluded that the average mass transfer Colburn factor (j_m) for the oval tube is 89% of that for the circular tube, while the average friction factor (f) for the oval tube is 46% of that for the circular tube. The ratio (j_m/f) for the oval tube is 1.93–1.96 times that for the circular tube. This means that the oval tube has a better combined thermal–hydraulic performance. The heat-mass transfer analogy showed lower values for the mass transfer coefficient estimated from dry heat transfer correlations when compared with wet measurements.

Keywords: Heat exchanger; Evaporative; Wet; Oval tube

1. Introduction

In an evaporatively cooled heat exchanger, heat transfer takes place from a hot fluid, flowing inside a tube, to a water film on the tube surface, and then to flowing air stream. The water film is formed by spraying water onto the surface of the tubes. The spray water is circulated in a closed circuit. The heat transfer from the water film to the forced flow air is in both sensible and latent

* Corresponding author. Tel.: +358-9-4513598; fax: +358-9-4513418.
E-mail address: ala.hasan@hut.fi (A. Hasan).

1359-4311/$ - see front matter
doi:10.1016/j.applthermaleng.2003.10.022

Nomenclature

a, b, B	constants
A	area (m^2)
C	specific heat of water ($J\,kg^{-1}\,K^{-1}$)
C_H	specific heat of moist air ($J\,kg^{-1}\,K^{-1}$)
D	for a circular tube: outside diameter, for an oval tube: outside diameter of a circular tube having equivalent perimeter (m)
Dif	Diffusivity ($m^2\,s^{-1}$)
h	enthalpy ($J\,kg^{-1}$)
$h'_a(\overline{t_s})$	saturated air enthalpy at the spray water temperature $\overline{t_s}$ ($J\,kg^{-1}$)
$h'_a(t_h)$	saturated air enthalpy at the hot water temperature t_h ($J\,kg^{-1}$)
k_a	air thermal conductivity ($W\,m^{-1}\,K^{-1}$)
k_x	convective mass transfer coefficient ($m\,s^{-1}$)
K_m	mass transfer coefficient ($kg\,s^{-1}\,m^{-2}$)
m	mass flow rate ($kg\,s^{-1}$)
r	radius (m)
t	temperature (°C)
$\overline{t_s}$	constant spray water temperature (°C)
U_o	overall heat transfer coefficient based on tube outside area ($W\,m^{-2}\,K^{-1}$)
v_{max}	air velocity at minimum section ($m\,s^{-1}$)

Greek symbols

α	convective heat transfer coefficient ($W\,m^{-2}\,K^{-1}$)
Γ	flow rate of spray water per unit breadth ($kg\,s^{-1}\,m^{-1}$)
θ	thermal performance parameter according to Eq. (12) (m^{-1})
μ	dynamic viscosity ($kg\,s^{-1}\,m^{-1}$)
ρ	density ($kg\,m^{-3}$)

Dimensionless numbers

f	friction factor, $f = \Delta p/(0.5\rho v_{max}^2)$
j_m	mass transfer Colburn factor, $j_m = K_m Sc^{2/3}/(\rho v_{max})$
Nu	Nusselt number, $Nu = \alpha_a D/k_a$
Re	Reynolds number, $Re = v_{max} D\rho/\mu$
Sc	Schmidt number, $Sc = \mu/(\rho\,\mathrm{Dif})$
Sh	Sherwood number, $Sh = k_x D/\mathrm{Dif}$

Subscripts

a	air
h	hot water
i	inside the tube
o	outside the tube
s	spray water
t	total

wb	wet-bulb
1	inlet to heat exchanger
2	outlet of heat exchanger

Superscripts

′	saturated condition
–	constant value

forms. The latent heat makes up a major part and is produced by the evaporation of a small amount of the spray water into the air stream, whereas the sensible heat is caused by the temperature gradient between the spray water and the air. Evaporatively cooled heat exchangers can achieve higher heat transfer rates than dry heat exchangers. Fig. 1 shows the arrangement of an evaporatively cooled heat exchanger.

The performance of two plain and finned circular tube evaporatively cooled heat exchangers was investigated in [1]. The heat and mass transfer coefficients were determined and the combined thermal–hydraulic performance was presented in terms of an energy index. The latter was found to be close for the two heat exchangers. It was concluded that the finned tubes make higher thermal utilisation of the volume with the same energy index.

If a heat exchanger is constructed from oval tubes (where the major axis is parallel to air flow), the expected air pressure drop will be low. This is due to the slender shape of an oval tube which has a smaller frontal area. The lower pressure drop will result in decreased pumping power required by the fan, which is the main source of energy consumption in an air cooled heat

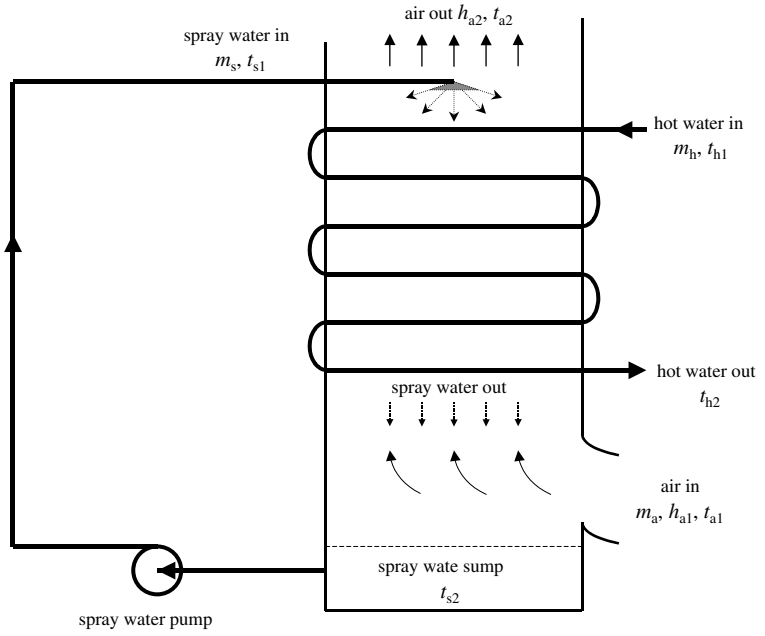

Fig. 1. Schematic of the evaporatively cooled heat exchanger.

exchanger. In addition, oval tubes can increase the compactness of heat exchangers as more tubes can fit into a specified volume. For dry heat exchangers, the published literature shows that the thermal behaviour of oval tubes has been subjected to investigation since the early work of Brauer [2] and Schulenberg [3]. There has been published very little about the utilisation of oval tubes in evaporatively cooled heat exchangers.

The objective of the current work is to compare, experimentally, the performance of plain circular and oval tubes in evaporatively cooled heat exchangers. The performance includes both the thermal and hydraulic behaviour. The experimental work is a continuation of the previous work [1] in which circular tubes were used. Here oval tubes are used under similar operating conditions so that differences in the performance will be as a result of the change in the tube shape.

2. Theory

The theory is based on the analysis presented in [1,4]. The analysis assumes a constant temperature $\overline{t}_s$ for the spray water in the heat exchanger. Fig. 2 shows the temperatures and enthalpies of the flowing streams and the direction of heat transfer. Following the direction of hot water flow, for an element dA_o around the tube surface, heat transfer dq from the hot water to the spray water is

$$dq = -m_h C\, dt_h = U_o(t_h - \overline{t}_s)\, dA_o \tag{1}$$

Integrating for the total outside surface area A_{ot} from the inlet to the outlet hot water temperatures, t_{h1} and t_{h2}, respectively, gives

$$\frac{U_o A_{ot}}{m_h C} = \ln\left(\frac{t_{h1} - \overline{t}_s}{t_{h2} - \overline{t}_s}\right) \tag{2}$$

where U_o is the overall heat transfer coefficient based on the total outside area of the tubes A_{ot}. The tube wall resistance is negligible, therefore

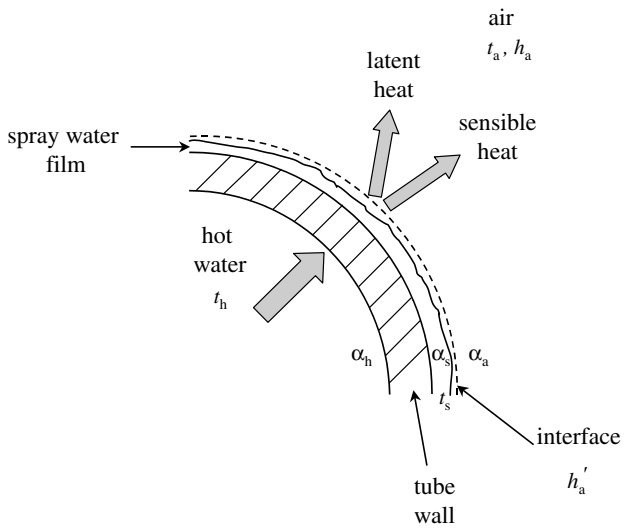

Fig. 2. Heat transfer from the tube.

$$\frac{1}{U_o} = \frac{1}{\alpha_h}\frac{r_o}{r_i} + \frac{1}{\alpha_s} \tag{3}$$

where α_h is the convective heat transfer coefficient between the hot water and the internal wall, and α_s is the convective heat transfer coefficient between the external wall and the spray water bulk.

The heat transfer resistance of the liquid side of the spray water–air interface could be assumed negligible, so that the interface temperature is taken at the spray water temperature $\overline{t_s}$. Heat gained by the air stream according to the Merkel equation [5] is

$$dq = -m_a\,dh_a = K_m(h'_a(\overline{t_s}) - h_a)\,dA_o \tag{4}$$

where $h'_a(\overline{t_s})$ is the saturated air enthalpy taken at the spray water temperature $\overline{t_s}$. Integrating from the inlet to the outlet air enthalpies, h_{a1} and h_{a2}, respectively, gives

$$\frac{K_m A_{ot}}{m_a} = \ln\left(\frac{h'_a(\overline{t_s}) - h_{a1}}{h'_a(\overline{t_s}) - h_{a2}}\right) \tag{5}$$

The coefficients U_o and K_m are overall heat and mass transfer coefficients, respectively.

For a constant spray water temperature, the total energy balance for the fluids flowing between the inlet and outlet of the heat exchanger gives

$$m_h C(t_{h1} - t_{h2}) = m_a(h_{a2} - h_{a1}) \tag{6}$$

In the current work, we will follow the same assumption which was made in [1], the constant spray water temperature $\overline{t_s}$ is taken to be equal to the measured inlet spray water temperature t_{s1} in the spray nozzle. This is due to the small vertical length of the heat exchanger which will result in small variation in the spray water temperature, and the influence of the end effects which will tend to cool the spray water.

The heat and mass transfer coefficients and h_{a1} are evaluated by solving Eqs. (2), (5) and (6) when the parameters (t_{h2}, h_{a2}, and $\overline{t_s}$) are fed from the measurements data, and the inlet operating conditions (m_h, m_a, and t_{h1}) and the geometry of the heat exchanger are specified.

2.1. Thermal and mass resistances

If the resistance to heat transfer (from the hot water to the spray water) and the resistance to mass transfer (from the spray water to the air) can be combined into one equation expressing the heat loss from the hot water, the relative effects of these resistances on the total heat loss can be concluded. The heat transfer resistance includes heat convection resistances between the hot water and the tube wall, and between the tube wall and spray water. The mass transfer resistance controls water vapour transfer from the air–spray water interface to the bulk air.

The relation between the saturation air temperature t'_a and the saturation air enthalpy h'_a can be approximated by a straight line, $h'_a = a + bt'_a$, where a and b are constants. For the operating temperature range implemented in the experiments, this equation shows less than 1% deviation in the air saturation enthalpy. Representing $h'_a(\overline{t_s})$, the saturated interface enthalpy at the spray water temperature $\overline{t_s}$, according to the linear saturation equation by $h'_a(\overline{t_s}) = a + b\overline{t_s}$. Substituting for $h'_a(\overline{t_s})$ in Eq. (4) gives

$$dq = K_m[(a + b\overline{t_s}) - h_a]\,dA_o \tag{7}$$

From Eq. (1) $\overline{t_s} = t_h - dq/(U_o\, dA_o)$, substituting by this for $\overline{t_s}$ in Eq. (7) and arranging the terms yields

$$dq = \frac{a + bt_h - h_a}{\dfrac{b}{U_o\, dA_o} + \dfrac{1}{K_m\, dA_o}} \tag{8}$$

Noting that $(a + bt_h)$ appearing in the numerator of this equation represents the air saturation enthalpy evaluated at the hot water temperature inside the tube t_h, which can be defined as $h'_a(t_h)$, hence

$$dq = \frac{[h'_a(t_h) - h_a]\, dA_o}{\dfrac{b}{U_o} + \dfrac{1}{K_m}} \tag{9}$$

The total heat transfer from the exchanger is determined by the integration of Eq. (9)

$$q = \frac{(\Delta h_a)_{lm} A_{ot}}{b\left(\dfrac{A_{ot}}{\alpha_h A_{it}} + \dfrac{1}{\alpha_s}\right) + \dfrac{1}{K_m}} \tag{10}$$

where A_{it} is the total inside area of the tubes, and $(\Delta h_a)_{lm}$ is the log-mean-air enthalpy-difference. The latter has a special definition in Eq. (10) as it refers to the difference between the air saturation enthalpy evaluated at the hot water temperature at the inlet and outlet of the heat exchanger, $h'_a(t_{h1})$ and $h'_a(t_{h2})$, and the corresponding air enthalpies at the same sections, h_{a2} and h_{a1}, respectively. The definition of $(\Delta h_a)_{lm}$ is

$$(\Delta h_a)_{lm} = \frac{\Delta h_{in} - \Delta h_{out}}{\ln(\Delta h_{in}/\Delta h_{out})} \tag{11}$$

where the differences are $\Delta h_{in} = h'_a(t_{h1}) - h_{a2}$ and $\Delta h_{out} = h'_a(t_{h2}) - h_{a1}$. Eq. (10) defines the heat transfer rate in terms of the $(\Delta h_a)_{lm}$ and the resistances to enthalpy transfer appearing in the denominator of the equation. The latter are consisted of the convective thermal resistances, on the internal and external wall surfaces, and the resistance to mass transfer from the interface.

3. Experimental work

The experimental system consisted of three circuits (air, hot water, and spray water). The test rig is the same one that was used to test the circular plain and finned tubes described in [1]. The reader can consult the aforementioned literature for information about the test rig. The results will be compared with those for the plain circular tube mentioned in the previous work [1].

3.1. Dimensions of oval tubes

Oval tubes are used instead of circular tubes in the heat exchanger. The oval tube was formed by heating and then pressing a circular copper tube in a proper mould. For the purpose of ease of

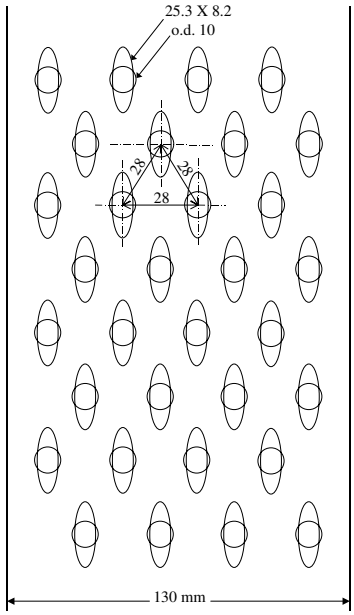

Fig. 3. Distribution of the circular and oval tubes in the test section.

manufacture, circular tubes having 18 mm o.d. were pressed into oval tubes. In the previous work, the heat exchanger was composed of 10 mm o.d. circular tubes. The formed oval tubes have a major axis of 25.3 mm, and a minor axis of 8.2 mm. The ratio of the axes is 3.085. The perimeter of the oval tube is equal to the perimeter of the circular tube from which it was formed. There are four oval tubes per each row, arranged in a staggered configuration, making eight rows. The horizontal tube length is 88 mm. The heat exchanger test cross-section is 88 mm × 130 mm, having a length of 250 mm. Fig. 3 shows the distribution of the oval tubes in the heat exchanger. The centres of the oval tubes coincide at the centres of the circular tubes from the previous work.

3.2. Test set-up data

The tests were conducted under operating conditions similar to those for the circular tubes in [1] (the same air and hot water flow rates, and nominal inlet cooling water temperatures) and as follows.

3.2.1. Air flow

Three airflow rates were considered: 0.0151, 0.0235, and 0.0323 $kg\,s^{-1}$, which were similar to those implemented for the circular tubes. Maximum air velocities in the minimum flow area were 1.47, 2.29, and 3.15 $m\,s^{-1}$, respectively. These velocities were about 8% lower than the corresponding values for circular tubes because of the relatively larger flow area between the oval tubes.

3.2.2. Hot water

The hot water flow rate was constant during the experiments and equal to 0.114 l s^{-1} (410 l h^{-1}). Three nominal inlet hot water temperatures (30, 32, and 34 °C) were considered.

3.2.3. Spray water

The spray water flow rate for the oval tubes was 0.0375 l s^{-1} (135 l h^{-1}). This flow rate was enough to wet the surfaces of the tubes. It was higher than that considered for the circular tubes 0.025 l s^{-1} (90 l h^{-1}). The reason for this is that in a horizontal cross-section of the heat exchanger, the oval tubes have smaller widths than the circular tubes which collect a smaller amount of spray water, therefore a higher spray water flow rate is required. The criterion was to ensure wetting of the surfaces of the tubes. It was observed during the measurements that the spray water fell from one tube to a lower tube in a droplet mode. The spray water Reynolds number from the circular tube measurements is in accordance with an empirical map indicated by Hu and Jacobi [6] for falling film in a quiescent surrounding for the droplet mode.

4. Results and discussion

4.1. Thermal performance of the tubes

To exclude the end-effect coming from the air–spray water contact in the lower end of the heat exchanger, air enthalpy is taken from the bottom of the tube bank to the air outlet when applying Eqs. (5) and (6).

The experimental measurements showed higher heat transfer rates for the oval tubes when compared with the circular tubes (10 mm o.d.) under similar air flow rates and with a similar temperature-difference potential at the inlet ($t_{h1} - t_{wb1}$). The latter represents the difference between the inlet hot water temperature t_{h1} and the outdoor air wet-bulb temperature t_{wb1}. The increase in the rate of heat transfer ranges from 36% to 61%, but it should be noted that the utilised oval tubes have 80% larger surface area.

An appropriate characteristic diameter D should be selected for the oval tubes. In the current work, D for the oval tube is taken equal to the outside diameter of a circular tube which has an equivalent perimeter. This is in accordance with a definition made by Ota et al. [7]. Here $D = 18$ mm.

To include the effect of the different surface areas for the oval and circular tubes, the heat flux could be considered. Furthermore, the effect of the outdoor wet-bulb temperature t_{wb1} could be considered by taking the temperature-difference potential at the inlet ($t_{h1} - t_{wb1}$). Therefore, a thermal performance parameter θ could be defined as

$$\theta = \frac{t_{h1} - t_{h2}}{(t_{h1} - t_{wb1})D} \tag{12}$$

This parameter is shown in Fig. 4 versus v_{max} the air velocity in the minimum flow area between the tubes for a dry section. Note that the hot water flow rate was constant during the experimental work so that ($t_{h1} - t_{h2}$) refers to the rate of heat transfer, and that the lengths of the tubes were equal, then $(t_{h1} - t_{h2})D^{-1}$ refers to the heat flux (heat transfer per surface area). It appears from

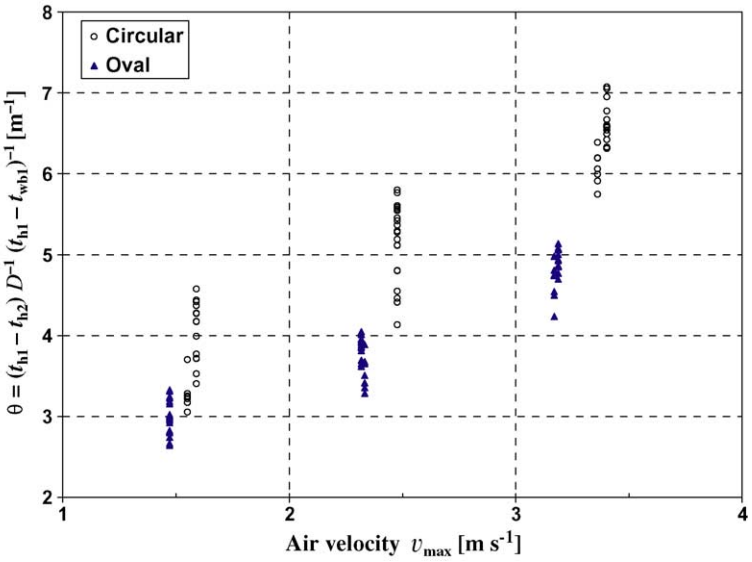

Fig. 4. Thermal performance parameter θ for the circular and oval tubes.

Fig. 4 that θ is lower for the oval tubes (on average it is 79% of that for the circular tube). Factors affecting the amount of heat transfer are: the temperature and enthalpy gradients, the hot water side heat transfer coefficient α_h, the spray water side heat transfer coefficient α_s, and the mass transfer coefficient between the spray water and the air K_m. The latter two coefficients are affected by the outer surface geometry of the tube and the air–water film interaction. For the circular tube, the larger frontal area and the higher turbulence induced on its backside will increase the rate of heat and mass transfer from the spray water film on the tube surface.

4.2. Heat and mass transfer coefficients

α_s and K_m are evaluated from the governing equations when the outlet conditions are fed as input data from the experimental measurements. The heat transfer coefficient between the tube surface and the spray water α_s is presented in Fig. 5. It shows that for a certain tube (circular or oval), α_s increases with the logarithmic temperature difference ratio for hot water $\ln[(t_{h1} - \overline{t_s})/(t_{h2} - \overline{t_s})]$. This is because as the latter term increases, U_o increases according to Eq. (2). It is noted from the measurement data that α_s is sensitive to $\overline{t_s}$, which was also seen in [1]. However, physically, there could only be minor dependence on $\overline{t_s}$. It is noted that $\ln[(t_{h1} - \overline{t_s})/(t_{h2} - \overline{t_s})]$ values for the oval tubes on the x-axis are shifted towards higher values. The reason for this is that, although the inlet operating conditions (t_{h1} and m_h) are constant, the higher surface area for the oval tubes results in higher rate of heat transfer, which causes t_{h2} to decrease and $\overline{t_s}$ to increase. This will increase the ratio $(t_{h1} - \overline{t_s})/(t_{h2} - \overline{t_s})$. Values of α_s for the oval tubes in Fig. 5 extend by an average of 12% higher values than that for the circular tubes. However, when taking into consideration the different tube diameters and spray water flow rates for the circular and oval tubes, the implementation of the equation by McAdams et al. [8], $\alpha_s = B(\Gamma/D)^{1/3}$, shows that α_s for the oval tubes

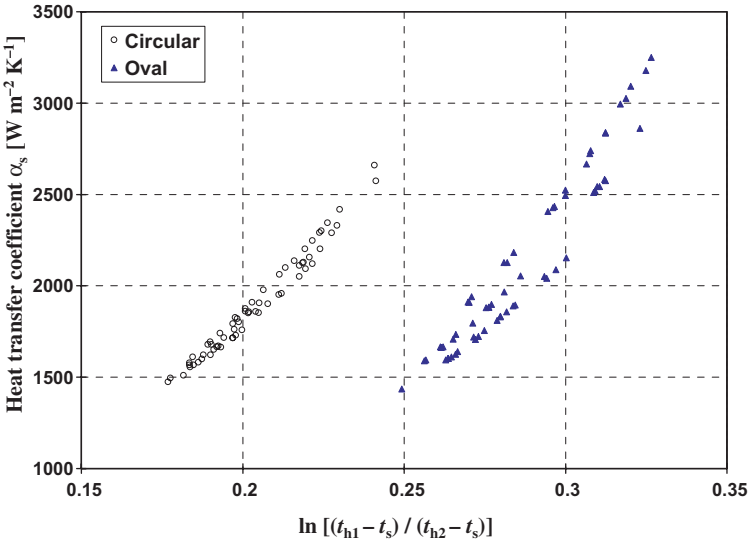

Fig. 5. Heat transfer coefficient α_s for the circular and oval tubes.

is 22% higher than that for the circular tubes. In this equation, B is a constant, and Γ is the spray water flow per unit breadth. It is assumed that D for the oval tube in this equation is the minor axis and that the entire amount of spray water falls onto the tubes.

The heat transfer rate from the hot water to the spray water is dependant on both α_s and α_h. The hot water flow area for the oval tube is 1.86 times the circular tube area. So, for the constant hot water flow rate, this means a corresponding lower hot water velocity. When the Gnielinski correlation [9] is implemented to estimate the heat transfer coefficient in the internal flow, it shows that α_h decreases by about 50% for the oval tube. Noting that α_s and α_h are of the same order of magnitude, the final effect is a decrease in the heat flux for the oval tube and as is shown by the thermal performance parameter θ in Fig. 4.

The mass transfer coefficients K_m concluded from the experimental measurements are shown in Fig. 6. Higher K_m values can be seen for the circular tubes. The distribution of K_m values is similar to those shown for the heat flux in Fig. 4. The data in Fig. 6 could be correlated in terms of airflow rate m_a: for the circular tubes $K_m = 3.36 m_a^{0.812}$, and for the oval tubes $K_m = 1.64 m_a^{0.706}$.

From the oval tubes measurements, the average value of K_m is 0.117 kg s^{-1} m^{-2} and the average value of U_o is 844 W m^{-2} K^{-1}. The effect of variation of K_m or U_o on the total heat transfer q can be determined from the differentiation of Eq. (10) with respect to K_m or U_o, respectively. From which we can find

$$\frac{dq/q}{dK_m/K_m} = \left(1 + \frac{bK_m}{U_o}\right)^{-1} \tag{13}$$

$$\frac{dq/q}{dU_o/U_o} = \left(1 + \frac{U_o}{bK_m}\right)^{-1} \tag{14}$$

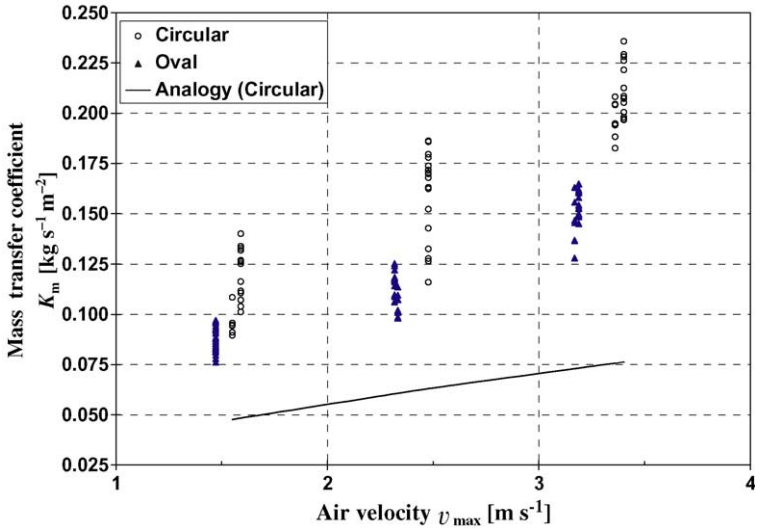

Fig. 6. Mass transfer coefficient K_m for the circular and oval tubes.

We can note that Eqs. (13) and (14) equal, respectively, the ratio of the mass transfer resistance and the heat transfer resistance, to the total resistance to enthalpy transfer and as indicated by Eq. (10). In Fig. 7, $(dq/q)/(dK_m/K_m)$ is plotted as a function of K_m from the measurements of the circular and oval tubes. It appears from this figure that the relative mass transfer resistance ranges from 48% to 70%. It can be concluded here that for our work, no general prediction could be made concerning which one is dominating, the mass transfer resistance or the heat transfer resistance. Despite that K_m appears to be relatively more effective, the exact effect is dependant on the value of the transfer coefficients for each case.

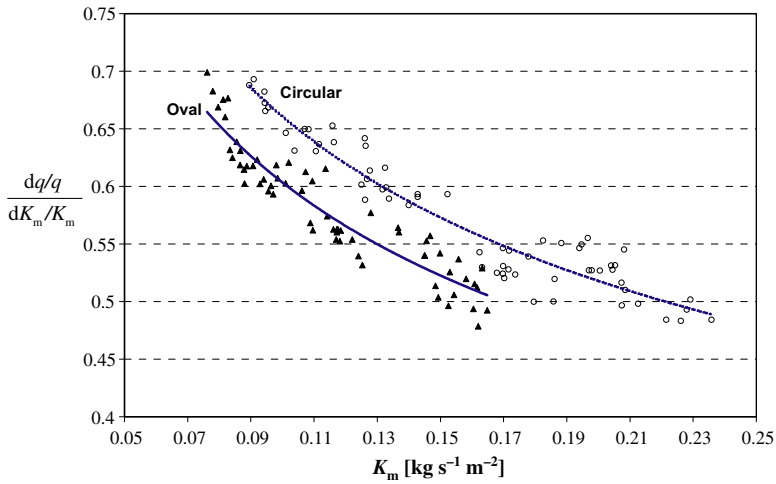

Fig. 7. The relative effect of variation of K_m on the total heat transfer from the experimental measurements.

4.3. Heat-mass transfer analogy

The heat-mass transfer analogy can be implemented to estimate the mass transfer coefficient K_m [10]. For circular tubes, correlations by Zhukauskas are presented in [9] for dry banks of staggered tubes in cross-flow. The correlations are in terms of the Nusselt number $Nu = \alpha_a D/k_a$, from which we can calculate α_a, the heat transfer coefficient between the dry tube surface and the air. The mass transfer coefficient K_m can be estimated from the Lewis relation $Le = \alpha_a/(K_m C_H)$, where C_H is the specific heat of moist air. K_m from the analogy is presented in Fig. 6. It is noticed that the analogy gives lower K_m values than those found from the measurements. This was also noticed by Parker and Treybal [11] and Dreyer and Erens [12], who indicated that the analogy would lead to low predictions for K_m. Such discrepancies could be attributed to a higher actual contact area produced by water splash and by interaction between the air–spray water film. In the current work it was noted that the internal surface of the casing was also wet.

One approximation could be made by assuming that the wet surfaces will include the internal casing area in addition to the surface area for the tubes. Assuming that all wetted surfaces are at a temperature $\overline{t_s}$, and that K_m is the same for the tubes and the casing surfaces. Therefore, new mass transfer coefficient from the measurements data could be calculated from Eq. (5). Fig. 8 presents the new K_m values and the analogy predictions. As a result, it is noted that the K_m values for the circular tube come closer to the analogy. We could not perform the analogy for the oval tubes because the literature lacks data for dry heat transfer from oval tubes having comparable axes ratio and tube spacing.

It should be noted that discrepancies between the measurement results and the heat-mass transfer analogy for a particular case would indicate different coefficients for the dimensionless groups from those available from the dry heat transfer correlations. This does not affect the validity of the Lewis relation.

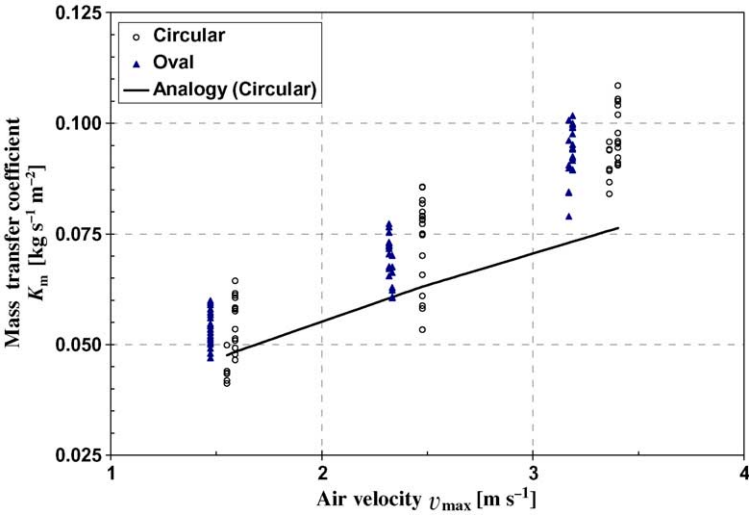

Fig. 8. Mass transfer coefficient K_m for the circular and oval tubes when including the internal casing area.

4.4. Combined thermal–hydraulic characteristics

According to our definition for the characteristic diameter D for an oval tube, the air Reynolds number Re will be higher for the oval tube despite that the air velocity v_{max} being close for the two types of tubes. The friction factor is calculated from the pressure drop measurements of air flow past the oval and circular tube banks in a dry operation. The friction factor f is defined as $f = \Delta p/(0.5\rho v_{max}^2)$, where Δp is the air pressure drop across one tube row. In Fig. (9), f from the measurement is shown versus the air Reynolds number Re, which indicates higher f values for the circular tubes. The data points of the parameters plotted in Fig. 9 are not shown in the figure for clarity.

The mass transfer Colburn factor j_m is defined as $j_m = Sh/(Re\,Sc^{1/3})$, where Sh is the Sherwood number and Sc is the Schmidt number. j_m can also be written as $j_m = K_m Sc^{2/3}/(\rho v_{max})$. The mass transfer Colburn factor j_m from the experimental measurements is plotted in Fig. 9 against the air Reynolds number Re for both the oval and circular tubes. The thermal–hydraulic characteristics of the tubes can be represented by the ratio of the mass transfer Colburn factor to the friction factor (j_m/f) which is also displayed in Fig. 9. It is concluded from this figure that the ratio (j_m/f) for the oval tubes is 1.93–1.96 times that for the circular tubes in the range of overlap of Re for the two types of tubes. The average Colburn factor for the oval tubes is 89% of that for the circular tubes. The main advantage comes from the lower friction factor for the oval tubes (f for the oval tubes is 46% of that for the circular tubes). This means that the oval tube requires lower energy than the circular one for air movement across the tube to accomplish a specified heat transfer duty.

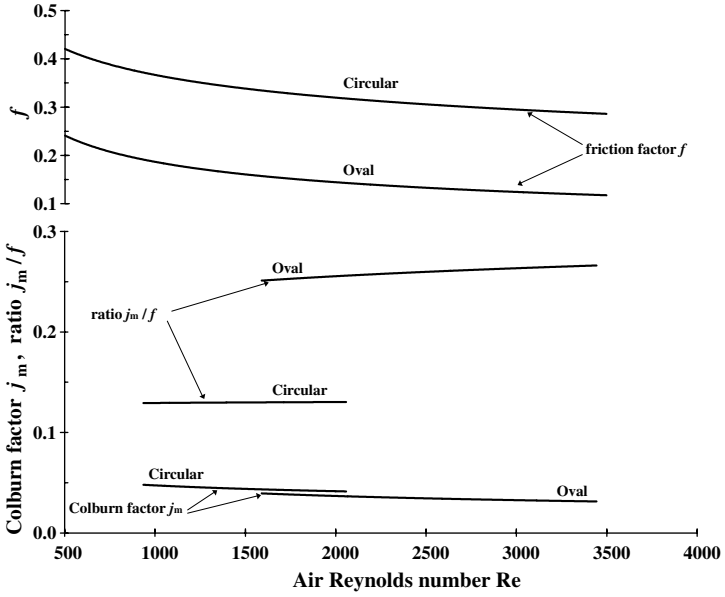

Fig. 9. Mass transfer Colburn factor j_m and friction factor f for the circular and oval tubes.

5. Conclusions

The thermal performance of the circular and oval tubes is compared per unit surface area per unit temperature-difference potential. The average performance parameter for the oval tube is 79% of that for the circular tube. The average mass transfer Colburn factor j_m for the oval tube is 89% of that for the circular tube, while the friction factor f for the oval tube undergoes a higher decrease when compared with the circular tube (f for the oval tube is 46% of that for the circular tube). Combining the thermal–hydraulic characteristics for the tubes, the oval tube shows higher values for the ratio (j_m/f) which is 1.93–1.96 times that for the circular tube.

The heat-mass transfer analogy showed lower values for the mass transfer coefficient estimated from dry heat transfer correlations when compared with wet measurements. The reason could be higher actual contact area between the air and the spray water.

It is concluded that the oval tube has good heat and mass transfer characteristics and better characteristics for the pressure drop, so that the combined heat–pressure performance shows favourable features for oval tubes in evaporatively cooled heat exchangers.

References

[1] A. Hasan, K. Sirén, Performance investigation of plain and finned tube evaporatively cooled heat exchangers, Applied Thermal Engineering 23 (3) (2003) 325–340.
[2] H. Brauer, Compact heat exchangers, Chemical and Process Engineering 45 (8) (1964) 451–460.
[3] F.J. Schulenberg, Finned elliptical tubes and their application in air-cooled heat exchangers, Transactions of the ASME 88 (1966) 179–190.
[4] A. Hasan, G. Gan, Simplification of analytical models and incorporation with CFD for the performance prediction of closed wet cooling towers, International Journal of Energy Research 26 (13) (2002) 1161–1174.
[5] F. Merkel, Verdunstungskuehlung, VDI Forschungsarbeiten No. 275, Berlin, 1925.
[6] X. Hu, A.M. Jacobi, The intertube falling film: Part 1—flow characteristics, mode transitions and hysteresis, Journal of Heat Transfer 118 (3) (1996) 616–625.
[7] T. Ota, H. Nishiyama, Y. Taoka, Heat transfer and flow around an elliptic cylinder, International Journal of Heat and Mass Transfer 27 (10) (1984) 1771–1779.
[8] W.H. McAdams, T.B. Drew, G.S. Bays, Heat transfer to falling-water films, ASME Transactions 62 (1940) 627–631.
[9] F.P. Incropera, D.P. DeWitt, Fundamentals of Heat and Mass Transfer, fourth ed., John Wiley, 1996.
[10] ASHRAE Fundamentals, American Society of Heating, Refrigeration and Air Conditioning Engineers, USA, 1997.
[11] R.O. Parker, R.E. Treybal, The heat-mass transfer characteristics of evaporative coolers, Chemical Engineering Progress Symposium Series 57 (32) (1962) 138–149.
[12] A.A. Dreyer, P.J. Erens, Heat and mass transfer coefficient and pressure drop correlations for a crossflow evaporative cooler, in: Proceedings of the Ninth International Heat Transfer Conference, vol. 6, Hemisphere Publ. Corp., New York, USA, 1990, pp. 233–238.